Korean J. Chem. Eng., 38(9), 1818-1825 (2021)
DOI: 10.1007/s11814-021-0833-1

pISSN: 0256-1115
eISSN: 1975-7220

Effect of hydroxyapatite-doping in Na-W-Mn/SiO_2 catalysts on oxidative coupling of methane

Byung Jin Lee*, Jae Hwan Lee*, Geun-Ho Han*, Young Gul Hur*,†, and Kwan-Young Lee*,,†**

*Department of Chemical and Biological Engineering, Korea University, 145, Anam-ro, Seongbuk-gu, Seoul 02841, Korea
**KU-KIST Green School, Korea University, 145, Anam-ro, Seongbuk-gu, Seoul 02841, Korea
(*Received 20 March 2021 • Revised 28 April 2021 • Accepted 29 April, 2021*)

Abstract−Sodium-tungsten-manganese supported on silica (Na-W-Mn/SiO_2) and hydroxyapatite (HAp) are representative catalysts for oxidative coupling of methane (OCM). In this work, the effect of the HAp doping in a Na-W-Mn/SiO_2 catalysts on the OCM performance was studied. To enhance the ethylene selectivity of the Na-W-Mn/SiO_2 catalyst, silica supports were coated with HAp containing hydroxyl and phosphate groups as oxygen species. A series of Na-W-Mn/xHAp_SiO_2 (x=1, 3, 5 and 7) catalysts with the different HAp coating cycles were prepared through the alternative soaking method, and X-ray diffraction (XRD) and scanning electron microscopy (SEM) showed that the amount of HAp doping was dependent on the HAp coating cycles. In addition, the change of oxygen species upon HAp doping was examined with X-ray photoelectron spectroscopy (XPS) and oxygen temperature-programmed desorption (O_2-TPD) techniques. With HAp doping, the increase of oxygen species assigned to metal oxide responsible for selective oxidation of methane to ethylene was observed in O 1s XPS spectra. In addition, weakly bound oxygen species were observed with the introduction of HAp doping in O_2-TPD profiles of prepared catalysts. The influence of these oxygen species on OCM catalytic performance was evaluated at an operating temperature of 775 °C and gas hourly space velocity of 18,000 ml/g_{cat}·h. The amount of HAp doping provided reactive oxygen species for oxidative dehydrogenation of ethane, which resulted in as much as 120% increase in C_2H_4/C_2H_6 ratio over the Na-W-Mn/3HAp_SiO_2 catalyst compared to the Na-W-Mn/SiO_2 catalyst.

Keywords: Oxidative Coupling of Methane (OCM), Na-W-Mn/SiO_2, Hydroxyapatite (HAp), Ethylene Selectivity, Oxidative Dehydrogenation of Ethane

INTRODUCTION

Methane (CH_4), one of the major greenhouse gasses, has been the cause of climate change [1]. The 'global warming potential (GWP)' can express the contribution of each greenhouse gas to the greenhouse effect, and methane has 21 times higher GWP than carbon dioxide. Hence, the elimination of methane is necessary, but simple combustion of methane can produce CO_2 which is another major greenhouse gas. As methane can be utilized as carbon source for synthesizing valuable chemicals such as methanol and ethylene, it can be eliminated through the conversion process. Thus, various conversion routes for production of chemicals from methane are meaningful and have been extensively investigated [2-4].

Methane conversion can be generally executed through chemical processes [5]. In the chemical conversion process, on the other hand, proper catalysts with energy like heat or plasma are used for the conversion of methane, and there are two routes using methane as a chemical feedstock: indirect and direct conversion pathways [2]. The indirect pathway begins by converting methane to synthetic gas (syngas, H_2/CO) via reforming reaction such as steam and dry reforming [4,6]. Then, syngas is used to synthesize platform chemicals like methanol, followed by olefin production via MTO (methanol-to-olefin) process. In the indirect conversion process, however, the installation costs for each of these reaction steps and separation/purification are considerable, and the removal of oxygen from CO of syngas to produce hydrocarbons is significantly difficult [3]. Methane, on the other hand, can be directly converted to valuable chemicals such as ethylene and aromatics by oxidative coupling of methane (OCM) and methane dehydroaromatization (MDA), respectively [3,7]. When is used directly, methane can be economically efficient in that an additional process is not necessary [8]. By increasing the yield of products, the direct pathway via simple one-step methane conversion process could potentially be more efficient and economically competitive than the indirect pathway.

Among the direct conversion of methane processes, OCM is used to directly synthesize C2 compounds such as ethylene (C_2H_4) and ethane (C_2H_6), crucial intermediates called 'building blocks' in a wide range of chemical industries, from methane [4,9-15]. It is highly challenging to convert the thermodynamically stable methane selectively to ethylene because the direction forming the by-products (CO, CO_2) is more favorable than the direction producing ethylene [16]. For these reasons, high operating temperature (above 700 °C) and suitable catalyst are required in the OCM reaction. Since 1982 when OCM was first reported, many researchers have devoted much effort into developing effective catalytic reaction systems [10,11,17-24]. Regarding OCM catalyst, sodium-tungsten-manganese supported on silica (Na-W-Mn/SiO_2), first reported by Li et al., is the most active catalyst, achieving methane conversion and C2 selec-

†To whom correspondence should be addressed.
E-mail: younggulhur@gmail.com, kylee@korea.ac.kr

tivity of 37.7% and 66.9%, respectively [25,26]. Despite high activity and stability of this catalytic system, the mechanism and characteristics of these catalysts are still not clear, but appropriate composition of each metal loading for maximum C2 yield has been suggested as 5 wt% Na_2WO_4 and 2 wt% Mn on SiO_2 support [11, 16,22,24,27].

In addition to Na-W-Mn/SiO_2 catalyst, other proposed OCM catalysts include lanthanum-based perovskite ($LaXO_3$; X=Al, Fe, or Ni) and hydroxyapatite ($Ca_{10}(PO_4)_6(OH)_2$; HAp) [28-32]. Among them, HAp, a non-stoichiometric calcium phosphate ceramic with a Ca/P molar ratio of 1.67 or less, has attracted attention as a promising OCM catalyst due to its thermal stability and ion exchange characteristics [19,21,28,30,31]. Also, there are two kinds of oxygen species in HAp, phosphate (PO_4^{3-}) and hydroxyl (OH^-) groups. Particularly, it was reported that the hydroxyl group in HAp is an active site for oxidative dehydrogenation of alkane [33].

As the HAp synthesis process is simple, it can be easily introduced to silica. To our best knowledge, the combination of these two materials, HAp and the Na-W-Mn/SiO_2 catalyst, has not been previously reported. To obtain an ethylene-selective catalyst, we have applied HAp doping to a Na-W-Mn/SiO_2 catalyst through the alternative soaking method and investigated the change of the oxygen species and its effect on the OCM catalytic activity [34].

EXPERIMENTAL

1. Catalyst Preparations

HAp coating on SiO_2 was performed by the alternative soaking method [34]. In this method, 2.0 g of silica gel (Sigma Aldrich, high-purity grade) was alternatively soaked in 16 ml of 0.2 M $CaCl_2$ (Sigma Aldrich, ≥99.99%) and 0.12 M Na_2HPO_4 (Sigma Aldrich, ≥99.0%) aqueous solutions. This alternative immersion was repeated 1, 3, 5 and 7 cycles. The samples were dried at 100 °C overnight and calcined at 800 °C for 3 h. According to the repeated HAp coating cycle, HAp-coated SiO_2 are denoted xHAp_SiO_2 (x=1, 3, 5, and 7). For comparison, HAp was prepared by the precipitation method with 1.0 M $Ca(NO_3)_2{\cdot}4H_2O$ (Sigma Aldrich, ≥99.0%) and 0.6 M $(NH_4)_2HPO_4$ (Sigma Aldrich, ≥99.99%). NH_4OH solution was added to maintain the pH of solution at 9. The precipitates were aged for 2 h at 80 °C and then washed with DI water and dried at 100 °C overnight. The dried samples were calcined at 800 °C for 3 h.

The tri-metallic catalysts (Na-W-Mn/SiO_2, Na-W-Mn/xHAp_-SiO_2, and Na-W-Mn/HAp) were prepared by the successive incipient wetness impregnation method. Na_2WO_4 (5 wt%) and Mn (2 wt%) were loaded on SiO_2, xHAp_SiO_2, and HAp with appropriate volume of aqueous precursor solutions containing $Na_2WO_4{\cdot}2H_2O$ (Sigma Aldrich, 99.995%) or $Mn(NO_3)_2{\cdot}4H_2O$ (Sigma Aldrich, 99.99%), respectively. After impregnation, prepared catalysts were dried at 100 °C overnight and calcined at 800 °C for 4 h. Before the activity tests, catalysts were sieved to obtain particles with sizes between 35 and 106 μm for a uniformly sized catalyst powder.

2. Catalyst Characterization

X-ray diffraction (XRD; SmartLab, Rigaku) with Cu Kα radiation (λ=0.154 nm) was performed at 45 kV and 200 mA to analyze the crystallinity of the prepared catalysts. The measurements were performed in the 2θ range 10-60° with a 2°/min of scanning rate. Inductively coupled plasma atomic emission spectroscopy (ICP-AES; HORIBA Jobin-Yvon, 123 Ultrace) was performed to quantify Na, W, Mn, Ca, and P content in the prepared catalysts. High resolution scanning electron microscopy (HR-SEM; Hitachi, SU-70) was performed to image the surface morphology of the catalysts. X-ray photoelectron spectroscopy (XPS; VG Microtech, ESCA 2000) was performed to investigate the surface concentration and chemical state of the catalytic components. XPS analysis was performed using an Al Kα X-ray source in an ultrahigh vacuum system. The C 1s binding energy at 284.6 eV was used as the reference. O_2-temperature programmed desorption (O_2-TPD; Microtrac BEL, Belcat-B) was performed to analyze the oxygen species. Before the measurements, the samples were heated to 800 °C and cooled to 100 °C in 10 vol% O_2/He balance gas. The gas flow was then switched to He gas and purged for 30 min to remove weakly bound oxygen species. After the pretreatment, the sample was heated to 950 °C at a ramp rate of 10 °C/min. ICP-AES and HR-SEM were performed at the Korean Basic Science Institute (KBSI) in Seoul, Republic of Korea.

3. Catalytic Reaction

In previous study, the OCM reaction system was described in detail [28]. Briefly, it was carried out in a fixed-bed reactor with an 8 mm inner diameter quartz-tube, and 0.1 g of the catalyst was placed on quartz wool at the middle of the reactor. CH_4 (99.995%), and O_2 (99.995%) were used as the reactant gases and N_2 (99.999%) was used as the internal standard gas. The reaction temperature was monitored with a K-type of thermocouple inserted in the catalyst bed. N_2 gas flowed at 15 ml/min until the temperature reached at 775 °C, and then reactant mixture gas was injected with 33.3 vol% CH_4, 16.7 vol% O_2, and 50.0 vol% N_2. The gas mixture was fed into the reactor at a total flow rate of 30 ml/min (gas hourly space velocity=18,000 ml/g_{cat}·h), regulated by mass flow controllers (Bronkhorst, EL-Flow classic). The byproduct of the OCM reaction (H_2O) was condensed through a cold trap (5 °C) connected to end of the quartz reactor. Product gases were analyzed by online gas chromatography (YoungLin, YL 6500) equipped with a flame ionization detector (FID) and a thermal conductivity detector (TCD) using a Gaspro capillary column and Carboxen 1000 packed column, respectively. Using the internal standard analysis method, the total flow, conversion of methane, and selectivity of the products were calculated based on the C1 basic [28].

RESULTS AND DISCUSSION

1. Formation of HAp on Na-W-Mn/xHAp_SiO_2 Catalysts

To investigate the HAp formation on SiO_2 through the alternative soaking method, XRD patterns of prepared supports without the impregnation of active metals are shown in Fig. S1. For amorphous SiO_2, only broad noise is observed. After three times and more HAp coating cycles (3HAp, 5HAp, and 7HAp_SiO_2), however, several peaks related to the HAp are observed, which indicates that the formation of HAp began from three cycles of coating [34,35]. With the increase of HAp coating cycles, these peaks become obvious, and the intensity monotonically increases. These results suggest that the formation of HAp on SiO_2 is dependent to HAp coating cycle. For 1HAp_SiO_2 sample, similar to amorphous SiO_2, only noise

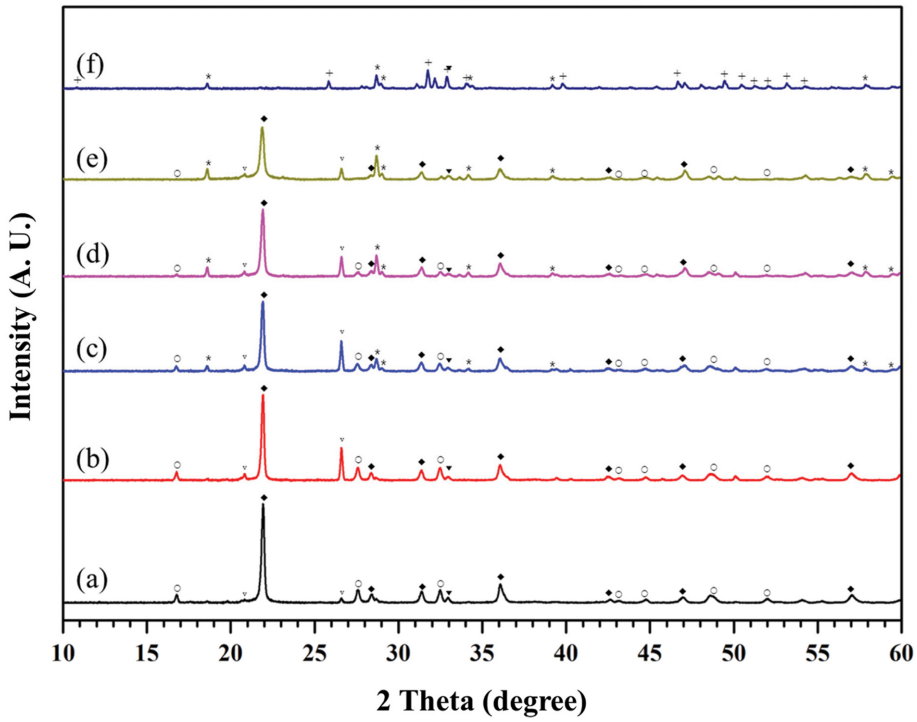

Fig. 1. XRD patterns of prepared samples (a) Na-W-Mn/SiO_2 (b) Na-W-Mn/1HAp_SiO_2 (c) Na-W-Mn/3HAp_SiO_2 (d) Na-W-Mn/5HAp_SiO_2 (e) Na-W-Mn/7HAp_SiO_2 (f) Na-W-Mn/HAp: (○) Na_2WO_4, (▼) Mn_2O_3, (◆) α-cristobalite, (v) quartz, (+) hydroxyapatite, (*) $CaWO_4$.

Table 1. Elemental analysis results of prepared samples

	Na	W	Mn	Ca	P	Ca/P ratio
Na-W-Mn/SiO_2	1.2	4.5	1.9	<0.1	<0.1	-
Na-W-Mn/1HAp_ SiO_2	1.4	4.2	1.7	0.3	0.3	1.00
Na-W-Mn/3HAp_ SiO_2	1.6	4.2	1.7	1.3	0.8	1.63
Na-W-Mn/5HAp_ SiO_2	1.6	4.0	1.4	2.2	1.3	1.69
Na-W-Mn/7HAp_ SiO_2	1.6	4.3	1.7	2.8	1.7	1.65
Na-W-Mn/HAp	1.2	4.2	1.4	41.3	19.9	2.08

is observed without any peaks for HAp, indicating that 1cycle of HAp coating is insufficient for the HAp formation.

After the impregnation of active metals (W, Mn), XRD patterns of prepared samples are shown in Fig. 1. For Na-W-Mn/SiO_2, Na-W-Mn/xHAp_SiO_2 (x=1, 3, 5, and 7) samples, Na_2WO_4, Mn_2O_3 are observed, suggesting that the active metals of prepared samples are properly impregnated on the prepared supports [11,13,15,18, 26]. Compared to XRD patterns in Fig. S1, the phase transition of SiO_2 from amorphous to crystalline such as α-cristobalite and quartz occurred with the introduction of active metals. It was reported that due to the interaction between sodium (Na) and SiO_2, the amorphous phase of SiO_2 is converted to crystalline at much lower temperature (800 °C) than normal transition temperature (1,500 °C) [17,36]. Also, for Na-W-Mn/xHAp_SiO_2 (x=3, 5 and 7) that HAp was formed, $CaWO_4$ as well as Na_2WO_4 are observed due to the interaction of Ca^{2+} and WO_4^{2-} [11]. Similarly, the diffraction patterns for HAp, $CaWO_4$, and Mn_2O_3 are observed over Na-W-Mn/HAp sample.

The elemental analysis results of prepared samples are shown in Table 1. For all prepared samples, the amounts of Na, W, and Mn impregnated as active metals are similar, 4.0-4.5 wt% of W and 1.4-1.9 wt% of Mn, regardless of used supports. These ranges correspond to the appropriate amounts of the active metals for the best OCM performance reported in several literatures [12,13,26,27]. Ca and P that compose the HAp structure are detected over Na-W-Mn/xHAp_SiO_2 (x=1, 3, 5, and 7) and Na-W-Mn/HAp samples, and the amount of these elements increases with the increase of HAp coating cycle. On the other hand, the Ca/P ratio can indirectly demonstrate the formation of HAp, and the appropriate ratio is in the range of 1.5-1.67, depending on the stoichiometric and non-stoichiometric HAp [28,37]. While Na-W-Mn/1HAp_SiO_2 sample shows 1.00 of Ca/P ratio, Na-W-Mn/xHAp_SiO_2 (x=3, 5, and 7) samples show the range of 1.63-1.69 of Ca/P ratios. This observation corresponds to the results of XRD patterns (Fig. S1) in which one cycle of HAp coating is not enough to form the HAp on the SiO_2, and the formation of HAp is strongly related to the number of HAp coating cycles. Meanwhile, the Ca/P ratio of Na-W-Mn/HAp, 2.08, is higher than the value of stoichiometric HAp,

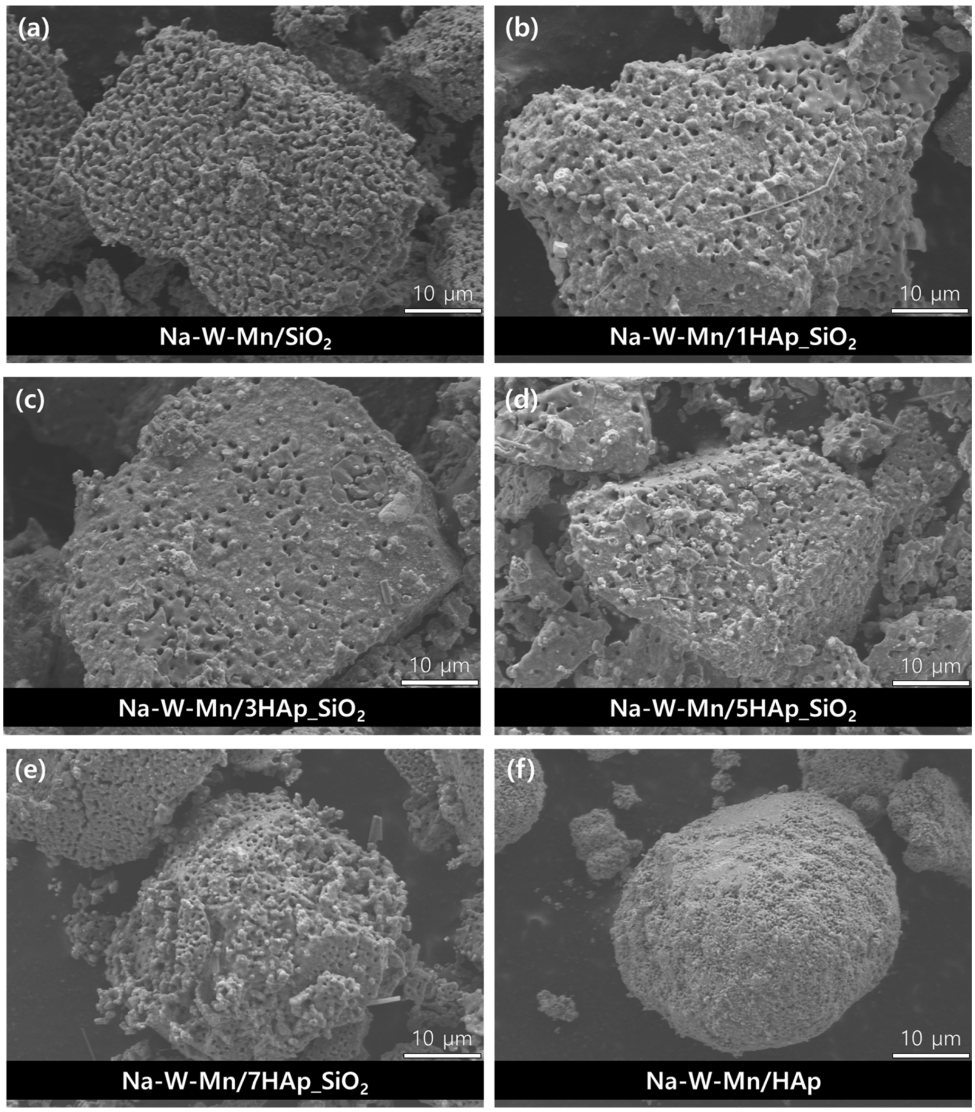

Fig. 2. SEM images of prepared samples.

Table 2. The observed XPS binding energies and near-surface composition of prepared samples

Catalysts	Na (1s)		W (4f)		Mn (2p)		Si (2p)		O (1s) (MO_x)		O (1s) (SiO_2)		Ca (2p)		P (2p)	
	BE (eV)	at. %	BE (eV)	at. %	BE (eV)	at. %	BE (eV)	at. %	BE (eV)	at. %	BE (eV)	at. %	BE (eV)	at. %	BE (eV)	at. %
Na-W-Mn/SiO_2	1,071.4	7.1	34.7	0.9	641.3	1.4	102.6	27.1	529.7	7.7	532.3	55.7	-	<0.3	-	<0.1
Na-W-Mn/1HAp_SiO_2	1,071.7	6.8	35.1	1.0	641.7	2.4	102.8	26.0	530.3	11.5	532.3	52.0	349.8	0.3	132.5	0.1
Na-W-Mn/3HAp_SiO_2	1,071.7	8.2	34.9	1.2	641.9	2.5	102.8	24.3	530.2	14.2	532.3	47.8	350.0	1.1	132.5	0.8
Na-W-Mn/5HAp_SiO_2	1,071.6	8.4	34.8	1.2	641.8	1.8	102.9	25.0	530.2	13.8	532.3	47.7	350.0	1.2	132.5	0.9
Na-W-Mn/7HAp_SiO_2	1,071.4	9.3	34.6	1.2	641.8	1.4	103.0	23.5	530.2	15.7	532.3	45.0	349.9	2.2	132.6	1.7
Na-W-Mn/HAp	1,071.6	7.3	34.5	2.4	641.5	2.6	0.0	0.0	530.6	60.2		0.0	350.2	15.8	132.8	11.7

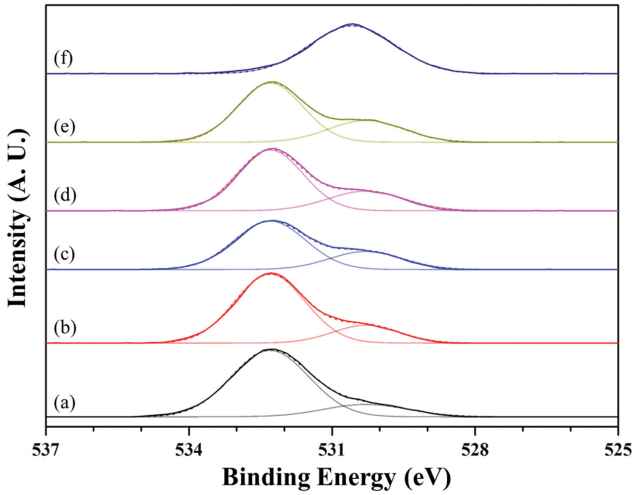

Fig. 3. The deconvoluted O 1s XPS spectra of prepared catalysts (a) Na-W-Mn/SiO_2 (b) Na-W-Mn/1HAp_SiO_2 (c) Na-W-Mn/3HAp_SiO_2 (d) Na-W-Mn/5HAp_SiO_2 (e) Na-W-Mn/7HAp_SiO_2 (f) Na-W-Mn/HAp.

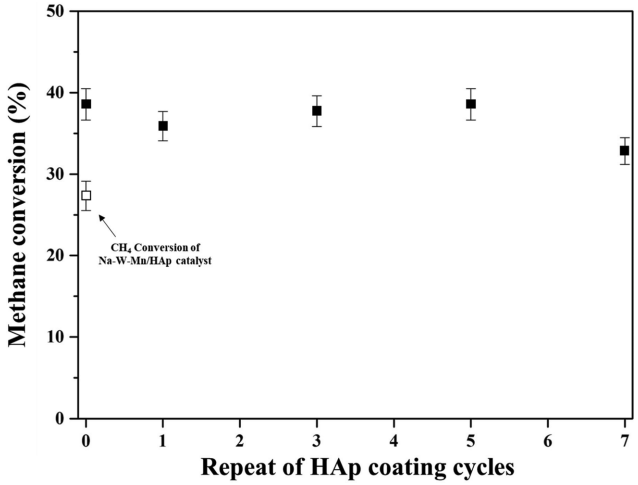

Fig. 4. Conversion of methane over prepared catalysts as a function of HAp coating cycles. Reaction condition: temp.=775 °C, GHSV=18,000 ml/g_{cat}·h, CH_4 : O_2 : N_2=2 : 1 : 1.

caused from the partial substitution of structural phosphate group to carbonate group in the precipitation process [38].

Regarding the surface morphology of catalysts, coral-like morphology is observed over Na-W-Mn/SiO_2 and Na-W-Mn/xHAp_-SiO_2 (x=1, 3, 5, and 7) because of the interaction between Na_2WO_4 and SiO_2 (Fig. 2(a)-(e)) [17]. As the HAp coating cycles increased, coral-like morphology became indistinct, suggesting that the interaction between Na_2WO_4 and SiO_2 is weakened with the increase of HAp formation. In addition, the type of HAp formed on SiO_2 through the HAp coating can be examined in SEM-EDS mapping images for Si element (Fig. S2). With the increase of HAp coating cycles, the number of black spots on the Si-mapping images tends to increase, and the location of black sites is identical to the sites that Ca and P are detected. It suggests that the HAp is formed on SiO_2 in the form of HAp doping, and HAp doping sites increase with the increase of HAp coating cycles. On the other hand, for Na-W-Mn/HAp sample that did not include SiO_2, the coral-like morphology is not observed (Fig. 2(f)).

Table 2 shows the observed binding energy and near-surface composition of prepared samples. For Na-W-Mn/SiO_2 and Na-W-Mn/xHAp_SiO_2 (x=1, 3, 5, and 7) samples, the near-surface concentrations of Na, W, and Mn are similar regardless of HAp doping, which indicates that impregnated elements were not affected by HAp doping. As shown in Table 2, however, oxygen species in prepared samples show a different trend with other elements. To examine the oxygen species, the O 1s XPS spectra are represented in Fig. 3. For Na-W-Mn/SiO_2 sample, the spectra can be deconvoluted into two kinds of peaks located at 532.3 and 530.0 eV, attributed to SiO_2 and metal oxides (MO_x), respectively [11-13]. With HAp doping, the peak related to MO_x tended to increase, and the near-surface concentration of MO_x increased (Table 2). Particularly, for Na-W-Mn/xHAp_SiO_2 (x=3, 5 and 7) samples that HAp doping was well formed, the near-surface concentration of MO_x is about twice higher than Na-W-Mn/SiO_2 sample. Since HAp included phosphate (PO_4^{3-}) and hydroxyl (OH^-) groups in the structure, HAp doping in prepared samples can quantitatively increase the oxygen species assigned to MO_x. As discussed in XRD and ICP results, the near-surface concentration of Ca and P is gradually increased with the increase of HAp coating cycles, which indicates that the extent of HAp doping increased with repeated HAp coating cycles. Therefore, it can be suggested that the increased oxygen species were attributed to the HAp formation. In OCM reaction, selective oxidation to ethylene is competitive with total oxidation to CO_x (CO, CO_2), and oxygen species in catalysts can determine the catalytic path. The oxygen species assigned to SiO_2 is not related to oxidation reaction, so that the other oxygen species attributed to MO_x can influence on the OCM activity of Na-

Table 3. The OCM activity of prepared catalysts. Reaction condition: temp.=775 °C, GHSV=18,000 ml/g_{cat}·h, CH_4 : O_2 : N_2=2 : 1 : 1

	CH_4 Conv.	Selectivity				Yield			C_2H_4/C_2H_6 ratio
		C2	C_2H_4	C_2H_6	CO_x	C2+	C_2H_4	C_2H_6	
Na-W-Mn/SiO_2	38.6	45.0	30.9	14.1	55.0	17.4	11.9	5.5	2.2
Na-W-Mn/1HAp_ SiO_2	35.9	43.8	31.8	12.0	56.2	15.7	11.4	4.3	2.7
Na-W-Mn/3HAp_ SiO_2	37.8	45.9	33.7	12.2	54.1	17.4	12.8	4.6	2.8
Na-W-Mn/5HAp_ SiO_2	38.6	41.6	30.3	11.3	58.4	16.1	11.7	4.4	2.7
Na-W-Mn/7HAp_ SiO_2	32.8	38.4	27.1	11.3	61.7	12.6	8.9	3.7	2.4
Na-W-Mn/HAp	29.7	24.3	17.8	6.5	75.7	7.2	5.3	1.9	2.7

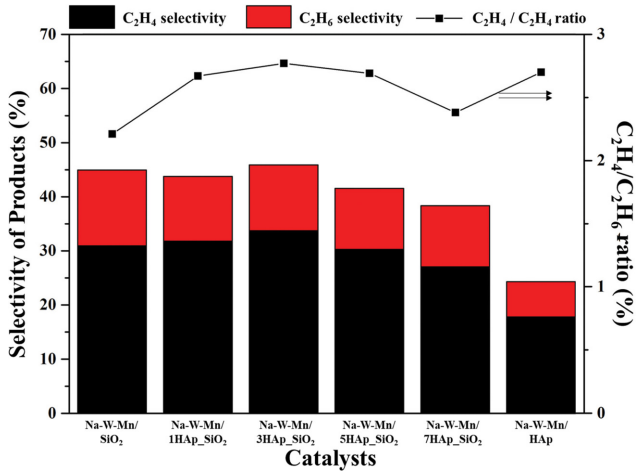

Fig. 5. Selectivity of ethylene (C_2H_4) and ethane (C_2H_6), and olefin/paraffin ratio (C_2H_4/C_2H_6) of prepared catalysts. Reaction condition: temp.=775 °C, GHSV=18,000 ml/g_{cat}·h, $CH_4 : O_2 : N_2$= 2 : 1 : 1.

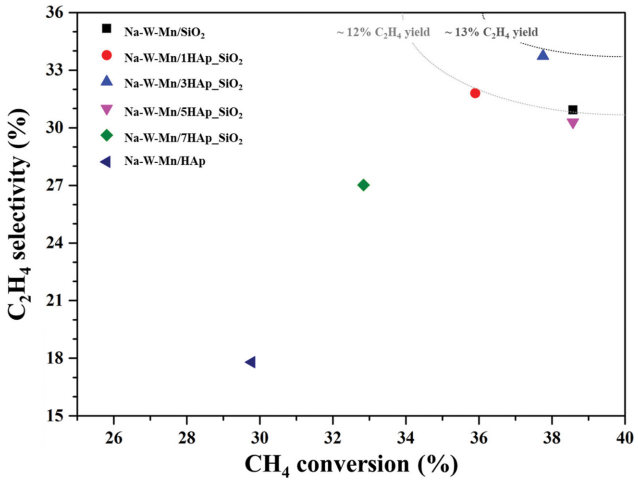

Fig. 6. OCM performance of prepared catalysts. Reaction condition: temp.=775 °C, GHSV=18,000 ml/g_{cat}·h, $CH_4 : O_2 : N_2$=2 : 1 : 1.

W-Mn/xHAp_SiO_2 catalysts [10,14,21].

2. Effect of HAp Doping on OCM Activity

The OCM reaction results are shown in Table 3 and Fig. 4, 5 and 6. As shown in Fig. 4, methane conversion is similar over Na-W-Mn/SiO_2 and Na-W-Mn/xHAp_SiO_2 (x=1, 3, and 5) catalysts at about 37.0%, whereas it slightly decreases to 32.8% over Na-W-Mn/7HAp_SiO_2 catalyst. Also, Na-W-Mn/HAp catalyst shows the lowest methane conversion at 29.7% among the prepared catalysts. It suggests that not only impregnated elements like W and Mn, but also support like SiO_2 can influence methane conversion [23]. The catalytic activity of SiO_2 in Na-W-Mn/7HAp_SiO_2 catalyst was partially obstructed by excessive HAp doping, and the methane conversion was reduced by 0.85 times compared to Na-W-Mn/SiO_2 catalyst.

The selectivity of produced C2 compounds including ethane (C_2H_6) and ethylene (C_2H_4), and the C_2H_4/C_2H_6 ratio is represented in Fig. 5. For Na-W-Mn/SiO_2 catalyst, C2 and C_2H_4 selectivity were 45.0% and 30.9%, respectively. Compared to Na-W-Mn/SiO_2 catalyst, Na-W-Mn/1HAp_SiO_2 and Na-W-Mn/3HAp_SiO_2 catalysts show similar C2 selectivity and slightly increased C_2H_4 selectivity (31.8% and 33.7%, respectively). For Na-W-Mn/5HAp_SiO_2 and Na-W-Mn/7HAp_SiO_2 catalysts, however, both C2 and C_2H_4 selectivity are lower than those for Na-W-Mn/SiO_2 catalyst. Particularly, Na-W-Mn/7HAp_SiO_2 catalyst shows 38.4% of C2 selectivity and 11.3% of C_2H_4 selectivity, 0.8 times that of Na-W-Mn/SiO_2 catalyst. In addition, C_2H_4/C_2H_6 ratio of Na-W-Mn/xHAp_SiO_2 catalysts (x=1, 3, 5, and 7) ranges from 2.4 to 2.8, which is higher than 2.2 of Na-W-Mn/SiO_2 catalyst. Particularly, Na-W-Mn/3HAp_SiO_2 catalyst shows 1.3 times higher value than Na-W-Mn/SiO_2 catalyst. These results imply that appropriate amount of HAp doping enhanced C_2H_4 selectivity, but excessive HAp doping has negative effect on C_2H_4 as well as C2 selectivity. Meanwhile, Na-W-Mn/HAp catalyst shows 24.3% of C2 selectivity and 17.8% of C_2H_4 selectivity; these are lowest values among the prepared catalysts, which indicates that SiO_2-supported catalysts are more appropriate for OCM reaction than HAp-supported one. To investigate the trend for the C_2H_4 yield, the combination of CH_4 conversion and C_2H_4 selectivity is depicted in Fig. 6. While Na-W-Mn/SiO_2, Na-W-Mn/1HAp_SiO_2, and Na-W-Mn/5HAp_SiO_2 catalysts show similar C_2H_4 yield at about 11%, Na-W-Mn/3HAp_SiO_2 catalyst shows the increased C_2H_4 yield to about 13%. However, for Na-W-Mn/7HAp_SiO_2 and Na-W-Mn/HAp catalysts, although the C_2H_4/C_2H_6 ratio are increased, the C_2H_4 yield is lower than Na-W-Mn/SiO_2 catalyst due to reduced C2 selectivity.

For the mechanism of OCM, the formation of C_2H_4 was proposed as a three step reaction (Scheme 1) [16,31,39]: First, CH_4 is activated to form a methyl radical (1). Then, C_2H_6 is formed from the coupling of two methyl radicals (2). Finally, C_2H_6 is converted to C_2H_4 through the oxidative dehydrogenation (3).

Scheme 1:

$$CH_4 \rightarrow CH_3\cdot + H\cdot \quad (1)$$

$$2CH_3\cdot \rightarrow C_2H_6 \quad (2)$$

$$C_2H_6 \rightarrow C_2H_4 + H_2 \quad (3)$$

Regarding the increased C_2H_4/C_2H_6 ratio with HAp doping, it is suggested that HAp doping influences step (3) in Scheme 1. As this reaction is oxidative dehydrogenation of C_2H_6 to C_2H_4, the hydrogen abstraction from C_2H_6 over the catalyst is important [33]. As mentioned in XPS results, HAp has two kinds of oxygen species, such as phosphate (PO_4^{3-}) and hydroxyl (OH^-) groups in the structure. It was reported that hydroxyl group of HAp contributes to the oxidative dehydrogenation of alkane by forming the reactive oxygen species [33]. With HAp doping, thus, reactive oxygen species was enhanced and this improved the oxidative dehydrogenation of C_2H_6, resulting in the higher C_2H_4/C_2H_6 ratio over Na-W-Mn/xHAp_SiO_2 catalysts. For Na-W-Mn/7HAp_SiO_2 catalyst, however, excessively increased reactive oxygen species improve not only oxidative dehydrogenation of C_2H_6, but also the total oxidation of produced C_2H_4 and C_2H_6 to CO_x.

Also, in order to examine the oxygen species of prepared catalysts, O_2-TPD was performed, and those profiles are represented in Fig. 7. For Na-W-Mn/SiO_2 catalyst, oxygen release begins at

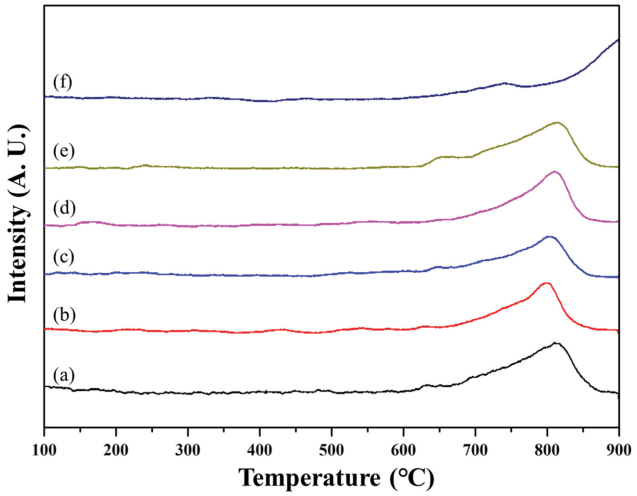

Fig. 7. O_2-TPD profiles of prepared catalysts (a) Na-W-Mn/SiO_2 (b) Na-W-Mn/1HAp_SiO_2 (c) Na-W-Mn/3HAp_SiO_2 (d) Na-W-Mn/5HAp_SiO_2 (e) Na-W-Mn/7HAp_SiO_2 (f) Na-W-Mn/HAp.

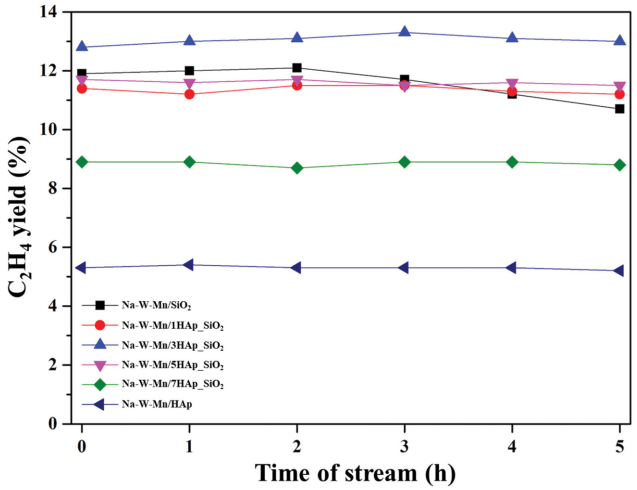

Fig. 8. C_2H_4 yield of prepared catalyst as a function of time. Reaction condition: temp.=775 °C, GHSV=18,000 ml/g_{cat}·h, CH_4 : O_2 : N_2=2 : 1 : 1.

around 600 °C, and the peak appears near 815 °C. For Na-W-Mn/xHAp_SiO_2 (x=1, 3, 5, and 7) catalysts, while the oxygen release begins at a similar temperature with that of Na-W-Mn/SiO_2 catalyst, the peak is observed at lower temperature of around 800 °C than that of Na-W-Mn/SiO_2 catalyst. However, the oxygen release for Na-W-Mn/HAp catalyst begins at around 600 °C and the peak is much higher over 900 °C than other catalysts. In OCM reaction, oxygen species of catalysts are responsible for the selective oxidation to C2 compounds and the total oxidation to CO_x [14,31]. As shown in Fig. 7, O_2-TPD profiles of Na-W-Mn/xHAp_SiO_2 (x=1, 3, 5, and 7) catalysts are shifted toward lower temperature range than that of Na-W-Mn/SiO_2 catalyst, indicating the weakly bound oxygen species increases with HAp doping. Sugiyama et al. reported that the reactive oxygen species, which is contributing to oxidative dehydrogenation of alkane, can be derived from the hydroxyl group in HAp [33]. Therefore, it can be suggested that the weakly bound oxygen species, observed in lower temperature range after HAp doping, are attributed from hydroxyl group of HAp. For these reasons, the C_2H_4/C_2H_6 ratio over HAp-doping catalysts is higher than Na-W-Mn/SiO_2 catalyst, suggesting that oxidative dehydrogenation of C_2H_6 is facilitated by the increased amount of reactive oxygen species. However, for Na-W-Mn/7HAp_SiO_2 catalyst, as HAp doping was excessively applied, the amount of reactive oxygen species excessively increased. Takanabe et al. reported that the oxidation of C_2H_4 over Na-W-Mn/SiO_2 catalyst is much easier than the oxidation of C_2H_6 and CH_4 [40]. For these reasons, for Na-W-Mn/7HAp_SiO_2 catalyst, it is suggested the oxidation of C_2H_4 to CO_x, which resulted in the decrease of C_2H_4 and increased of CO_x selectivity, respectively. Hence, appropriate HAp doping provides Na-W-Mn/SiO_2 catalyst with more reactive oxygen species and improves the selective oxidation to C_2H_4 in OCM reaction.

In addition, as shown in Fig. 8, HAp doping on Na-W-Mn/SiO_2 catalyst improves not only the C_2H_4 yield, but also the stability of catalysts. For Na-W-Mn/SiO_2 catalyst, the yield of C_2H_4 began to decrease after 2 h, and it became about 0.85 times of the initial yield after 5 h of reaction. For Na-W-Mn/xHAp_SiO_2 (x=1, 3, 5, and 7) catalysts, however, the C_2H_4 yield was stably maintained for 5 h of reaction, which suggests that thermally stable HAp enhances the stability of catalysts.

CONCLUSIONS

In order to enhance the C_2H_4 selectivity in OCM, HAp coating was applied to Na-W-Mn/SiO_2 catalysts through alternative soaking, and HAp was introduced as a form of doping. The amount of HAp doping is quantitatively dependent on the number of HAp coating cycles, and HAp containing the hydroxyl and phosphate group provides reactive oxygen species to Na-W-Mn/xHAp_SiO_2 catalysts. In terms of qualitative oxygen species, the hydroxyl group in HAp, reported as reactive oxygen species in oxidative dehydrogenation of alkane, facilitates the oxidative dehydrogenation of C_2H_6 to C_2H_4, which results in the increased C_2H_4/C_2H_6 ratio in Na-W-Mn/xHAp_SiO_2 catalysts. Hence, Na-W-Mn/3HAp_SiO_2 catalyst shows higher C_2H_4 yield than Na-W-Mn/SiO_2 catalyst. However, excessive HAp doping in Na-W-Mn/7HAp_SiO_2 catalyst improves not only the oxidative dehydrogenation of C_2H_6, but also the oxidation of C_2H_4 to CO_x, which results in the decrease of C2 selectivity. Thus, the proper amount of HAp doping on Na-W-Mn/xHAp_SiO_2 catalysts effectively converts the CH_4 to C_2H_4 with enhanced C_2H_4 selectivity compared to Na-W-Mn/SiO_2 catalyst.

ACKNOWLEDGEMENTS

This research was supported by the C1 Gas Refinery Program through the National Research Foundation of Korea (NRF) and funded by the Ministry of Science and ICT (2021M3D3A1A010 22109).

SUPPORTING INFORMATION

Additional information as noted in the text. This information is

available via the Internet at http://www.springer.com/chemistry/journal/11814.

REFERENCES

1. Y. Kathiraser, Z. Wang and S. Kawi, *Environ. Sci. Technol.*, **47**, 14510 (2013).
2. K. Takanabe, *J. Jap. Petrol. Inst.*, **55**, 1 (2012).
3. P. Schwach, X. Pan and X. Bao, *Chem. Rev.*, **117**, 8497 (2017).
4. R. Horn and R. Schlögl, *Catal. Lett.*, **145**, 23 (2015).
5. P. J. Strong, S. Xie and W. P. Clarke, *Environ. Sci. Technol.*, **49**, 4001 (2015).
6. O. Shtyka, M. Zakrzewski, R. Ciesielski, A. Kedziora, S. Dubkov, R. Ryazanov, M. Szynkowska and T. Maniecki, *Korean J. Chem. Eng.*, **37**, 209 (2020).
7. B. J. Lee, Y. G. Hur, D. H. Kim, S. H. Lee and K.-Y. Lee, *Fuel*, **253**, 449 (2019).
8. S. H. Lee, J. K. Kang and E. D. Park, *Korean J. Chem. Eng.*, **35**, 2145 (2018).
9. Y. Gambo, A. Jalil, S. Triwahyono and A. Abdulrasheed, *J. Ind. Eng. Chem.*, **59**, 218(2018).
10. J. Wu, S. Li, J. Niu and X. Fang, *Appl. Catal. A: Gen.*, **124**, 9 (1995).
11. S. Ji, T. Xiao, S. Li, L. Chou, B. Zhang, C. Xu, R. Hou, A. P. York and M. L. Green, *J. Catal.*, **220**, 47 (2003).
12. S.-f. Ji, T.-c. Xiao, S.-b. Li, C.-z. Xu, R.-l. Hou, K. S. Coleman and M. L. Green, *Appl. Catal. A: Gen.*, **225**, 271 (2002).
13. J. Wang, L. Chou, B. Zhang, H. Song, J. Zhao, J. Yang and S. Li, *J. Mol. Catal. A: Chem.*, **245**, 272 (2006).
14. Y. Gordienko, T. Usmanov, V. Bychkov, V. Lomonosov, Z. Fattakhova, Y. Tulenin, D. Shashkin and M. Sinev, *Catal. Today*, **278**, 127 (2016).
15. Y. T. Chua, A. R. Mohamed and S. Bhatia, *Appl. Catal. A: Gen.*, **343**, 142 (2008).
16. R. T. Yunarti, S. Gu, J.-W. Choi, J. Jae, D. J. Suh and J.-M. Ha, *ACS Sustain. Chem. Eng.*, **5**, 3667 (2017).
17. Q. Yan, Y. Wang, Y. Jin and Y. J. Chen, *Catal. Lett.*, **13**, 221 (1992).
18. A. Malekzadeh, A. Khodadadi, A. Dalai and M. Abedini, *J. Nat. Gas Chem.*, **16**, 121 (2007).
19. S.-H. Lee and K. J. Yoon, *Korean J. Chem. Eng.*, **18**, 228 (2001).
20. G. Keller and M. Bhasin, *J. Catal.*, **73**, 9 (1982).
21. K. Y. Lee, Y. C. Han, D. J. Suh and T. J. Park, *Stud. Surf. Sci. Catal.*, **119**, 385 (1998).
22. S. Arndt, T. Otremba, U. Simon, M. Yildiz, H. Schubert and R. Schomäcker, *Appl. Catal. A: Gen.*, **425-426**, 53 (2012).
23. T. W. Elkins and H. E. Hagelin-Weaver, *Appl. Catal. A: Gen.*, **497**, 96 (2015).
24. C. Uzunoglu, A. Leba and R. Yildirim, *Appl. Catal. A: Gen.*, **547**, 22 (2017).
25. X. Fang, S. Li, J. Lin and Y. Chu, *J. Mol. Catal. (China)*, **6**, 427 (1992).
26. Z. C. Jiang, C. J. Yu, X. P. Fang, S. B. Li and H. L. Wang, *J. Phys. Chem.*, **97**, 12870 (1993).
27. S. Gu, H.-S. Oh, J.-W. Choi, D. J. Suh, J. Jae, J. Choi and J.-M. Ha, *Appl. Catal. A: Gen.*, **562**, 114 (2018).
28. J. H. Park, D.-W. Lee, S.-W. Im, Y. H. Lee, D.-J. Suh, K.-W. Jun and K.-Y. Lee, *Fuel*, **94**, 433 (2012).
29. D. Kwon, I. Yang, Y. Sim, J.-M. Ha and J. C. Jung, *Catal. Comm.*, **128**, 105702 (2019).
30. K. Y. Lee, M. Houalla, D. M. Hercules and W. K. Hall, *J. Catal.*, **145**, 223 (1994).
31. S. C. Oh, Y. Lei, H. Chen and D. Liu, *Fuel*, **191**, 472 (2017).
32. I. Kim, G. Lee, H. B. Na, J.-M. Ha and J. C. Jung, *Mol. Catal.*, **435**, 13 (2017).
33. S. Sugiyama and H. Hayashi, *Int. J. Mod. Phys. B*, **17**, 1476 (2003).
34. K. Suzuki, T. Yumura, M. Mizuguchi, T. Taguchi, K. Sato, J. Tanaka and M. Akashi, *J. Sol-Gel Sci. Technol.*, **21**, 55 (2001).
35. P. Li, I. Kangasniemi, K. De Groot, T. Kokubo and A. Yli-Urpo, *J. Non-Cryst. Solids*, **168**, 281 (1994).
36. A. Palermo, J. P. H. Vazquez, A. F. Lee, M. S. Tikhov and R. M. Lambert, *J. Catal.*, **177**, 259 (1998).
37. J. Elliott, *Structure Chemistry of the Apatites and Other Calcium Orthophosphates: Hydroxyapatite and Nonstoichiometric Apatites*, **18**, 111 (1994).
38. M. Domínguez, F. Romero-Sarria, M. Centeno and J. Odriozola, *Appl. Catal. B: Environ.*, **87**, 245 (2009).
39. A. Galadima and O. Muraza, *J. Ind. Eng. Chem.*, **37**, 1 (2016).
40. K. Takanabe and E. Iglesia, *Angew. Chem. Int. Ed.*, **120**, 7803 (2008).

Supporting Information

Effect of hydroxyapatite-doping in Na-W-Mn/SiO_2 catalysts on oxidative coupling of methane

Byung Jin Lee*, Jae Hwan Lee*, Geun-Ho Han*, Young Gul Hur*,†, and Kwan-Young Lee*,,†**

*Department of Chemical and Biological Engineering, Korea University, 145, Anam-ro, Seongbuk-gu, Seoul 02841, Korea
**KU-KIST Green School, Korea University, 145, Anam-ro, Seongbuk-gu, Seoul 02841, Korea
(*Received 20 March 2021 • Revised 28 April 2021 • Accepted 29 April, 2021*)

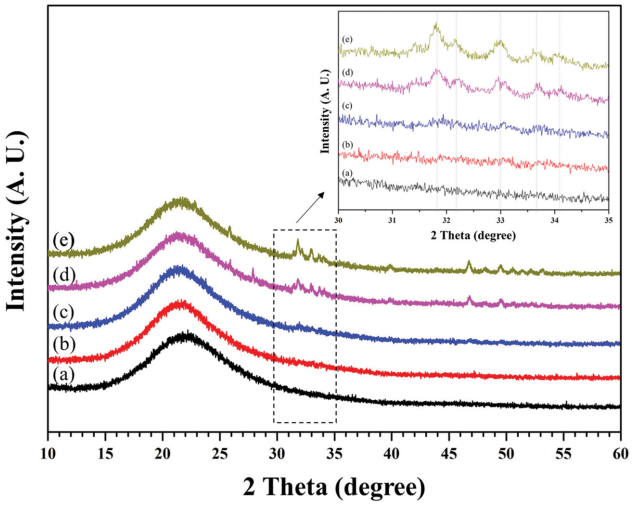

Fig. S1. XRD pattern of (a) SiO_2 and (b)-(e) xHAp (x=1, 3, 5 and 7). The inserted image is the enlarged XRD patterns in the range of 30-35°.

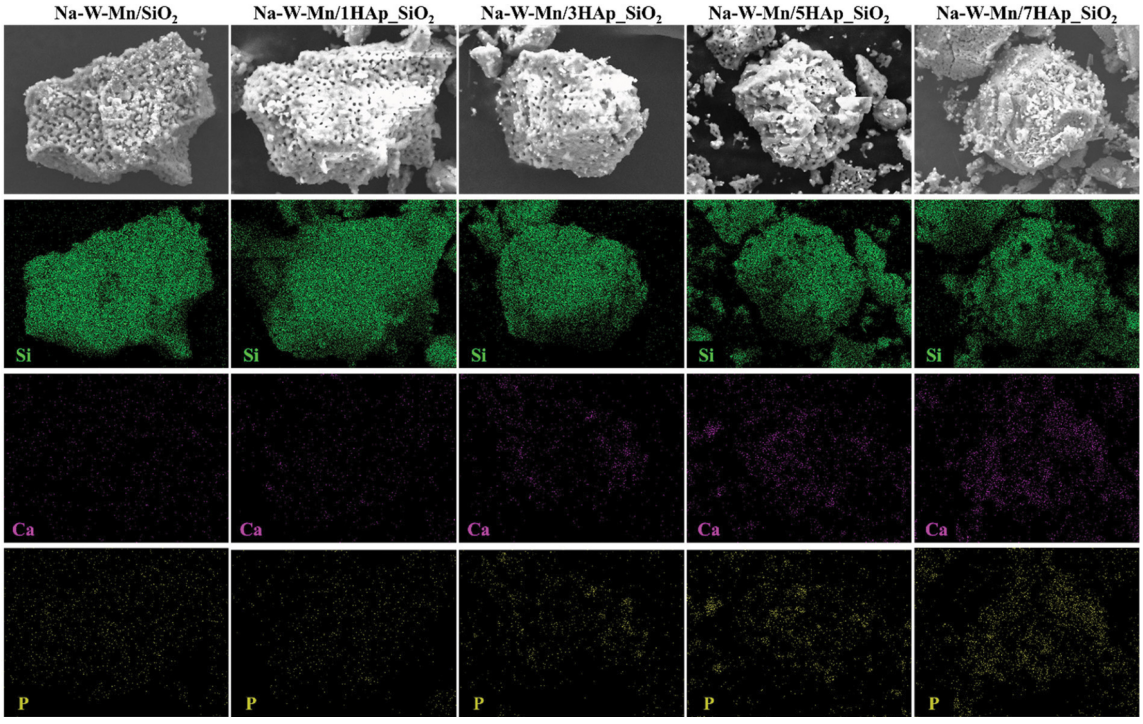

Fig. S2. SEM and EDS mapping images of prepared samples.